LETTER

A new model of the L–H transition in tokamaks

Nucl. Fusion **52** (2012) 062003 (8pp) doi:10.1088/0029-5515/52/6/062003

LETTER

A new model of the L–H transition in tokamaks*

W. Fundamenski[1,2], **F. Militello**[1], **D. Moulton**[2] **and D.C. McDonald**[1]

[1] Culham Centre for Fusion Energy, Abingdon, UK
[2] Imperial College of Science, Technology and Medicine, London, UK

E-mail: wojtek.fundamenski@ccfe.ac.uk and wfundamenski@gmail.com

Received 1 December 2011, accepted for publication 27 February 2012
Published 24 April 2012
Online at stacks.iop.org/NF/52/062003

Abstract
A new model of the L–H transition in tokamaks is proposed, based on the criterion that the transition occurs when plasma turbulence and shear Alfvén waves compete in the vicinity of the last-closed flux surface. The model is used to predict the scaling of the H-mode access power, $P_{\mathrm{L–H}}$, with magnetic and plasma variables. The predictions are in good agreement with the experimental scaling of $P_{\mathrm{L–H}}$ with plasma size, density, magnetic field and edge safety factor (plasma current). They are also qualitatively consistent with the dependence of $P_{\mathrm{L–H}}$ on ion mass and charge, limiter versus divertor plasmas, single versus double null configurations, the divertor leg length and H–L versus L–H hysteresis. Most notably, the model explains the appearance of the minimum in $P_{\mathrm{L–H}}$ with plasma density (in terms of the transition between sheath limited and conduction limited scrape-off layer (SOL) transport) and correctly predicts the scaling of the density minimum with magnetic field and Greenwald number. Finally, the effect of toroidal field reversal is included by making the normalized correlation length of the eddy and maximum safety factor in the edge-SOL layer functions of $\boldsymbol{B} \times \nabla B$ direction.

(Some figures may appear in colour only in the online journal)

Access to the high confinement (H-mode) regime is critical for the commercial viability of fusion energy by magnetic confinement, especially for tokamaks, e.g. ITER[3]. Yet, after more than a quarter of a century since the discovery of the H-mode on the ASDEX tokamak [1], an adequate model of the L–H (low-to-high confinement) transition is yet to be developed, despite multiple attempts [2–4]. Needless to say, such a model would be highly desirable. Since auxiliary heating power is expensive, and hence limited, the principle task of any model of the L–H transition is to reproduce and explain the variation of the minimum power for accessing the H-mode, $P_{\mathrm{L–H}}$, with the main engineering quantities, such as the observed scaling of $P_{\mathrm{L–H}}$ with the toroidal magnetic field, B, the plasma (electron) density, n_{e}, and the plasma surface area, $S_{\perp}$, at medium to high density [5],

$$P_{\mathrm{L–H}} \propto B^{0.803\pm0.03} n_{\mathrm{e}}^{0.717\pm0.04} S_{\perp}^{0.94\pm0.02} \tag{1}$$

and the (relatively weak) variation with the cylindrical safety factor,

$$q_{\mathrm{cyl}} = 2\pi\epsilon\kappa a B/(\mu_0 I_{\mathrm{p}}). \tag{2}$$

Moreover, the dependence on additional parameters (inverse aspect ratio, ϵ, ion mass, A, and charge, Z, the poloidal field topology, and scrape-off layer (SOL) and divertor geometry, toroidal field direction, etc) should also be reproduced. In this letter, we propose a new model of the L–H transition, which can explain the functional dependence of $P_{\mathrm{L–H}}$ on most of the above factors[4]. The model does not address the subsequent edge transport barrier evolution, saturation and relaxation, and is hence only a partial explanation of the H-mode phenomenon.

As our starting ansatz, we postulate that the L–H transition is mainly a consequence of edge plasma dynamics, and that it

[3] While the H-mode has also been found on helical devices, e.g. stellarators, we recognize that such plasmas include additional variables linked to helical rather than axis-symmetry and to the presence of complicated separatrix structures. As such, we limit the present discussion exclusively to H-mode in tokamaks.

[4] We purposely use the term 'model' as opposed to 'theory', to emphasize the mathematical rather than a physical nature of the model, i.e. we do not propose a new set of physical mechanisms but rather a new set of relationships between known mechanisms.

* This letter is an intended contribution to the upcoming *Nuclear Fusion* special issue: H-MODE.

begins in the edge region, in close vicinity of the last-closed flux surface (LCFS) and/or the ideal magnetic separatrix, i.e.

$$0 < (r_{\rm LCFS} - r_\star)/L_{\rm p} \ll 1, \tag{3}$$

where r is the radial co-ordinate, $r_{\rm LCFS}$ is its value on the LCFS (i.e. $r_{\rm LCFS} = a$, where a is the minor radius), and $L_{\rm p} \approx |\nabla_\perp p/p|^{-1}$ is the mean pressure gradient length. In other words, we postulate that the L–H transition depends on *local* magnetic field structure and *local* plasma parameters and their gradients.

Next, we conjecture that the L–H transition occurs when the parallel Alfvenic time in the edge region becomes comparable to the perpendicular transport time, as defined below. Since this criterion is central to the model, we introduce a new dimensionless number, which we shall refer to as the *Wagner number*, Wa, to express it[5]. Hence, the L–H transition occurs when Wa exceeds some critical value, $Wa_{\rm L-H}$, which is a constant of comparable to unity,

$$\tau_\parallel^A/\tau_\perp^Q \equiv Wa > Wa_{\rm L-H} = {\rm const} \sim 1. \tag{4}$$

In this definition,

$$\tau_\parallel^A \equiv L_\parallel(r_\star)/V_A(r_\star) \tag{5}$$

is the Alfvénic time at the radial location, $r_\star$, of the L–H transition, and

$$\tau_\perp^Q \equiv L_\perp^{\rm corr}(r_\star)/V_\perp^Q(r_\star) \tag{6}$$

is the perpendicular electron energy transport time at $r_\star$ over a radial correlation length of a turbulent eddy. In (5) and (6), $L_\parallel$ is the parallel connection length, $V_{\rm A}$ is the Alfvén velocity, $L_\perp^{\rm corr}$ is the radial correlation length, and $V_\perp^Q$ is the radial velocity of electron energy transport.

This is the core hypothesis of the model, since it expresses a *criterion* for the L–H transition. In tokamak plasmas, which can be described as stratified drift-hydrodynamics (DHD), we would expect the Alfvén waves to play an important role in drift-wave turbulence; indeed, it is now generally accepted that drift-Alfvén wave turbulence driven by radial pressure gradients is the dominant radial transport channel in the edge plasma under L-mode conditions [8, 9]. Indications of this role have been recognized since the early days of magnetized plasma physics and span from Kadomtsev [10], who described the linear coupling between the drift and Alfvén waves, to the works of Scott [11] and Rogers *et al* [12], in which drift-wave induced turbulent transport in the edge is shown to be significantly affected by electromagnetic effects. A recurring theme is the strong coupling of these waves as their characteristic times become comparable. When this happens, the electron response is no longer adiabatic and a robust nonlinear drift-wave instability can occur. This, in turn, can enhance the *inverse energy cascade*[6], leading to $E \times B$ velocity shears associated with zonal flows and, as a consequence, to turbulence quenching.

In other words, a new channel becomes available at the transition, in which the energy of the turbulence can flow and be redirected to harmless (from the confinement point of view) axisymmetric perturbations, i.e. the coupling between drift and Alfven waves, occurring when the Wagner number approaches unity, favours an inverse energy cascade which leads to the formation of zonal flows[7] [23]. The standard paradigm of the zonal flow–drift-wave interaction can be understood as a follows: (i) zonal flows are generated by drift-wave nonlinearity, and then (ii) zonal flows react back on the turbulent flow by tilting the turbulent eddies via their velocity shear. This results in a reduction of the radial correlation length of the eddies (thus reducing the perpendicular transport) but not in a significant change in their poloidal correlation length. This is consistent with observations on tokamaks, e.g. [2], in which the poloidal correlation length shows no significant change between L-mode and H-mode. Finally, an important consequence of zonal flows is the augmented radial electric field, as typically observed during the L–H transition, e.g. [2], although the details of the zonal flow and radial electric field generation are outside the scope of the present model.

The above ideas have motivated several previous theories of the L–H transition, e.g. by [15, 16], none of which, however, propose the L–H criterion as (4) (nor any equivalent form), nor do they introduce the concepts of magnetic field stochasticity and SOL parallel transport as key elements of the transition. In contrast, we will show that the two effects enter our proposed L–H criterion, (4) via $L_\parallel$ in (5), and via both $L_\perp^{\rm corr}$ and $V_\perp^Q$ in (6), respectively, without otherwise modifying the physics of the transition.

It is worth noting that (4) represents the condition of *critical balance* between the rates of eddy deformation in the $\parallel$ and $\perp$ directions in magnetohydrodynamic (MHD) turbulence. When this condition is satisfied, the turbulent cascade occurs preferentially within the 2D drift plane, which in tokamaks would give rise to the inverse energy cascade needed for zonal flow formation [6, 7]. Moreover, in stratified MHD Alfvén waves can stabilize the R-T instability if the Alfvénic time is shorter than the interchange time [7], i.e. when (4) is *violated*! This would imply more robust turbulence levels when (4) is *satisfied*, which once again could be channelled into zonal flow via the inverse energy cascade.

Our next task is to obtain expressions for $L_\parallel$, $L_\perp^{\rm corr}$ and $V_\perp^Q$ which appear in (5) and (6). To estimate $L_\parallel$ in the vicinity of the separatrix one needs to consider the nature of the magnetic field in the edge region of divertor tokamaks. Classical mechanics [17] and the KAM theorem [18] predict the separatrix to be a fragile object, i.e. unstable to tiny perturbations. This fragile object, on which ideally $L_\parallel \propto q_{sep} \to \infty$, breaks up into a thin stochastic layer, in which the magnetic field has a 3D structure, see figure 1. As a result, q_{sep} saturates at some finite value, which scales weaker than linearly with $q_{\rm cyl}$ [19].

Due to the presence of the stochastic layer, we may assume $q_\star \equiv q(r_\star)$ to scale weaker than linearly with the plasma current, e.g. with a square-root dependence,

$$q_\star \approx \alpha_\star q_{\rm cyl}^{1/2}, \qquad L_\parallel^\star \approx \pi q_\star R, \tag{7}$$

[5] This is first usage of this term, which we name in honour of Fritz Wagner, who first observed the H-mode on the Asdex tokamak, see [1].

[6] This refers to a cascade of turbulent kinetic energy from small to large scales, in contrast to the *direct energy cascade* from large to small scales. The former is caused by conservation of enstrophy (vorticity) and is hence a characteristic of 2D turbulent flows (in both neutral fluids and plasmas), whereas the latter involves vortex stretching and is hence a feature of 3D turbulence, see [6, 13, 14].

[7] Recall that zonal flows axis-symmetric meso-scale objects that naturally arise from the drift-wave turbulence.

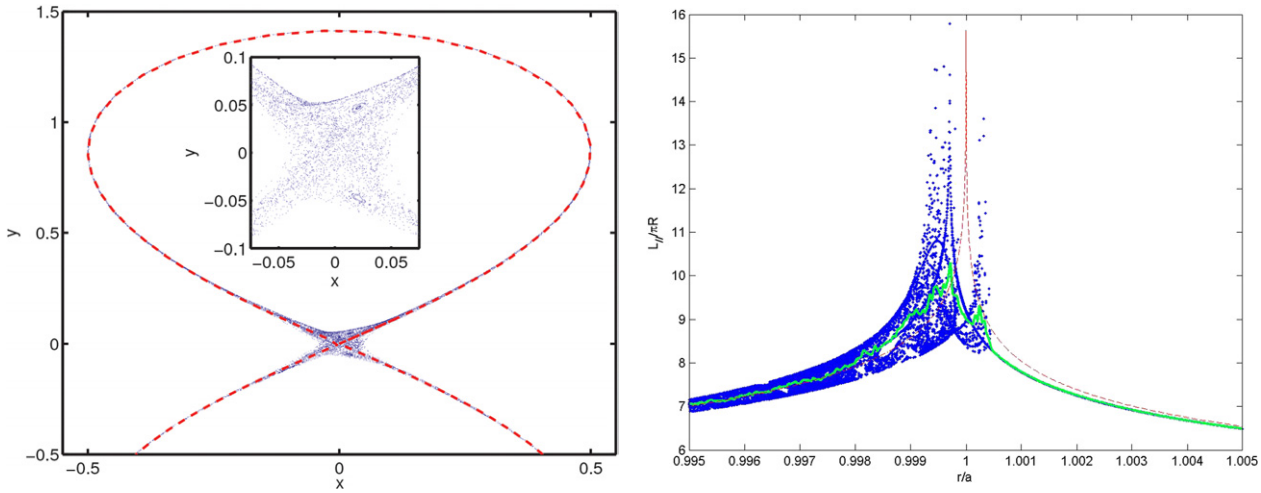

Figure 1. Left frame: Poincaré plot of the near-separatrix stochastic region based on a Hamiltonian vacuum field calculation. The dashed line shows the position of the unperturbed separatrix. In the inset, a zoom of the X-point region is shown; right frame: the related 'safety factors' (blue points), defined as $q = \Delta\phi/2\pi \approx L_\parallel/\pi R$, where $\Delta\phi$ is the toroidal angle subscribed for one poloidal rotation and $L_\parallel$ is the corresponding parallel distance, in the vicinity of the separatrix, as well as their mean values for axis-symmetric (red dashed line) and perturbed (green diamonds) cases.

where $\alpha_\star > 1$ is a free parameter in the model and $L_\parallel^\star \approx \pi q_\star R$ is the parallel length (half a poloidal turn) at $r_\star$. Since the effect of the magnetic perturbation is likely to be much weaker on the open field lines, we assume that the safety factor in the near SOL, $q_\odot$ is linear proportional to $q_{\rm cyl}$,

$$q_\odot \approx \alpha_\odot q_{\rm cyl}, \qquad L_\parallel^\odot \approx \pi q_\odot R. \tag{8}$$

where $\alpha_\odot \approx 1$ is a free parameter and $L_\parallel^\odot$ is the connection length in the near-separatrix SOL.

We estimate the radial correlation length of a turbulent eddy in the edge region (shear-layer) as some multiple of the meso-scale,

$$L_\perp^{\rm corr} \approx \alpha_\perp \sqrt{L_{\rm p}\rho_{\rm S}}, \tag{9}$$

where $\alpha_\perp \sim 1$ is a free parameter in the model. The meso-scale consists of a logarithmic average of the mean pressure gradient length in the edge region, $L_{\rm p}$, and the ion gyro-radius evaluated at the plasma sound speed, $\rho_{\rm S}$,

$$\rho_{\rm S} = \frac{C_{\rm S}}{\Omega_i} = \sqrt{\frac{ZT_{\rm e}+T_{\rm i}}{m_{\rm i}}}\left(\frac{m_{\rm i}}{ZeB}\right) \approx \frac{\sqrt{T_{\rm e}}}{e\zeta B} \propto \sqrt{\frac{AT_{\rm e}}{Z}}\frac{1}{B}. \tag{10}$$

Here again we assume a two species plasma with $n_{\rm e} = Zn_{\rm i}$, $T_{\rm e} = T_{\rm i}$ and $m_{\rm i} = Am_{\rm p}$, so that $\zeta = \sqrt{Z/Am_{\rm p}}$. It is worth stressing that the estimate (9) is consistent both with current thinking on the nature of edge-SOL turbulence as well as with experimental data, e.g. recent measurements on JET [20][8].

Guided by combination of physical insight (expected dominance of turbulent convective transport in the edge region[9]) and empirical evidence ($L_{\rm p}$ increases roughly linearly with size and decreases roughly linearly with plasma current), we assume that $L_{\rm p}$ scales linearly with a and the local safety factor, $q_\star$,

$$L_{\rm p}^\star \equiv L_{\rm p}(r_\star) \propto aq_\star A^{-1/2} \propto R\epsilon q_{\rm cyl}^{1/2} A^{-1/2}, \tag{11}$$

where $\epsilon = a/R$ is the inverse aspect ratio, with typical $L_{\rm p}/a \approx 0.025$. This is consistent with the observations on JET [21], TCV [22] and across many machines [23]. The additional mass scaling is motivated by the mean free path of neutrals (penetration), which increases as neutral thermal velocity, and hence as $1/\sqrt{A}$ [24].

The radial velocity of electron energy transport, $V_\perp^Q$, appearing in (6), is estimated as

$$V_\perp^Q \equiv Q_\perp/(\frac{3}{2}p_{\rm e}) \equiv P_\perp/[\frac{1}{2}S_\perp \times \frac{3}{2}p_{\rm e}], \tag{12}$$

where $P_\perp$ is the power crossing the flux surface (assumed to exit over the outboard surface area), and $p_{\rm e} = n_{\rm e}T_{\rm e}$ is the electron pressure. At $r = r_\star \approx a$, these become

$$P_\perp \approx P_\odot, \quad S_\perp \approx 4\pi^2 R^2 \epsilon\sqrt{\kappa}, \quad p_{\rm e} = p_{\rm e}(r_\star), \tag{13}$$

where $P_\odot = P_{\rm heat} - P_{\rm rad}^{\rm core}$ is the power entering the SOL and κ is the plasma elongation.

The L–H transition criterion, (4), together with the estimate of $V_\perp^Q(r_\star)$ (12) now yields an expression for the L–H access power,

$$P_{\rm L-H} \approx \frac{3}{4}p_{\rm e\star}S_\perp V_{A\star}L_\perp^{\rm corr\star}/L_\parallel^\star, \tag{14}$$

with all terms evaluated at $r_\star$. Recalling that the Alfvén speed is defined as

$$V_{A\star} \equiv \frac{B}{\sqrt{m_{\rm i}n_{\rm i\star}}} = \frac{B\zeta}{\sqrt{n_{\rm e\star}}} \propto \frac{B}{\sqrt{n_{\rm e\star}}}\sqrt{\frac{Z}{A}}. \tag{15}$$

Using (7), (9), (10) and (11) to provide expressions for $L_\parallel^\star$, $L_\perp^{\rm corr}$, $\rho_{\rm S}$ and $L_{\rm p}^\star$, we find the following scaling:

$$P_{\rm L-H} \propto (n_{\rm e\star}B\kappa/q_\star)^{\frac{1}{2}}(R\epsilon)^{\frac{3}{2}}Z^{\frac{1}{4}}A^{-\frac{1}{2}}T_{\rm e\star}^{\frac{5}{4}}, \tag{16}$$

[8] Basically, the free energy driving the edge-SOL turbulence comes mainly from the edge pressure gradients (not from the SOL)! Empirically, $L_{\rm p}$ is fairly continuous across the separatrix, so the exact location at which it is to be evaluated makes little practical difference in the model, but it is important for the physical interpretation.

[9] This suggests the following scaling for $L_{\rm p}$ in the edge plasma: $L_{\rm p} \sim V_\perp\tau_\parallel \sim M_\perp C_{\rm S}(L_\parallel/C_{\rm S}) \sim M_\perp aq_\star \sim aq_\star$.

which suggests a critical role played by electron temperature (consistent with many observations, e.g. [25]).

To approximate the temperature and density at the L–H transition location, i.e. at $r_\star \approx r_{\rm LCFS} - \delta L_{\rm p}$, where δ is a small number, see (3), we take their near-separatrix SOL values, i.e. at $r_\odot \approx r_{\rm LCFS} + \delta L_{\rm p}$. In effect, we assume that the relative variation of $n_{\rm e}$ and $T_{\rm e}$ across a layer of thickness $\Delta = \delta L_{\rm p}$ is small. This is supported by vacuum field simulations (performed specifically for this purpose, see figure 1), which suggest that the stochastic magnetic field has maximum $L_\parallel \propto q$ in a layer of width $\Delta = 10^{-3} r_{\rm LCFS}$ inside the separatrix. Since $L_{\rm p}$ is typically $\approx 0.02 r_{\rm LCFS}$, this implies that $\Delta/L_{\rm p} = \delta \approx 0.05 \ll 1$ as required. The above assumption permits us to use the so-called two-point model of SOL transport [7, 26], to estimate the electron temperature and density at $r_\odot$ as the 'upstream' SOL values in the two-point model, using

$$T_{\rm eu}^{7/2} \approx T_{\rm et}^{7/2} + \frac{7}{4} P_\odot L_\parallel^\odot / (S_\parallel \kappa_{0\rm e}), \tag{17}$$

where $T_{\rm eu}$ and $T_{\rm et}$ are the upstream and target values of the temperature and $\kappa_{0\rm e} \propto A^0 Z_{\rm eff}^{-1} \sim Z^{-1}$ is a constant in the Spitzer–Harm expression for parallel heat conduction, $\kappa_{\parallel \rm e} = \kappa_{0\rm e} T_{\rm e}^{5/2}$ [27, 28]. This relation follows directly from a quadrature of the parallel electron heat conduction equation,

$$P_\odot / S_\parallel = Q_{\parallel \rm e} \approx \kappa_{\parallel \rm e} \nabla_\parallel T_{\rm e} = \kappa_{0\rm e} T_{\rm e}^{5/2} \nabla_\parallel T_{\rm e}, \tag{18}$$

between the upstream and target regions.

The target temperature in (17) may be obtained by invoking two additional assumptions of the two point model: (i) pressure conservation, $n_{\rm u} T_{\rm u} \approx 2 n_{\rm t} T_{\rm t}$, and (ii) the target energy flux boundary condition,

$$P_\odot / S_\parallel = Q_{\parallel \rm t} = \gamma T_{\rm et} n_{\rm et} C_{\rm St}, \Rightarrow T_{\rm et} \approx \left(P_\odot / S_\parallel \gamma \zeta n_{\rm et} \right)^{2/3} \tag{19}$$

where $\gamma = \gamma_{\rm e} + \gamma_{\rm i} \approx 8$ is the total sheath energy transmission coefficient. The parallel energy flow (cross-sectional surface) area, $S_\parallel$, may be derived from a divergence form of energy conservation, $\nabla_\parallel Q_\parallel \approx \nabla_\perp Q_\perp$,

$$S_\parallel = S_\perp (L_\perp / L_\parallel)_\odot \approx 4\pi R \sqrt{\kappa} \lambda_Q \epsilon / q_\odot. \tag{20}$$

where $\lambda_Q = |\nabla_\perp Q_\parallel / Q_\parallel|^{-1} \approx \int Q_\parallel \, {\rm d}r / Q_{\rm max}$ is the radial power width in the SOL.

Finally, the power e-folding length in the near-separatrix SOL, appearing in (20), is estimated as

$$\lambda_Q \approx V_\perp \tau_{\parallel Q}, \tag{21}$$

where $V_\perp$ is the effective radial transport velocity and

$$\tau_{\parallel Q} \approx \tau_{\parallel T} \approx L_\parallel^2 / \chi_{\parallel \rm e}, \quad \chi_{\parallel \rm e} \sim v_{\rm te} \lambda_{\rm ei} \tag{22}$$

is the parallel energy removal time, which is assumed here to be dominated by parallel electron conduction. Defining $M_\perp^\odot = V_\perp / C_{\rm S} \approx$ const as the perpendicular Mach number and $\nu_\odot = L_\parallel^\odot / \lambda_{\rm ei} \propto Z n_{\rm eu} L_\parallel^\odot / T_{\rm eu}^2$ as the plasma collisionality in the upstream SOL near the LCFS, then (21) and (22) may be combined to yield

$$\lambda_Q \propto q_\odot R (Z/A)^{1/2} \nu_\odot M_\perp^\odot \propto R q_{\rm cyl} (Z/A)^{1/2} \nu_\odot. \tag{23}$$

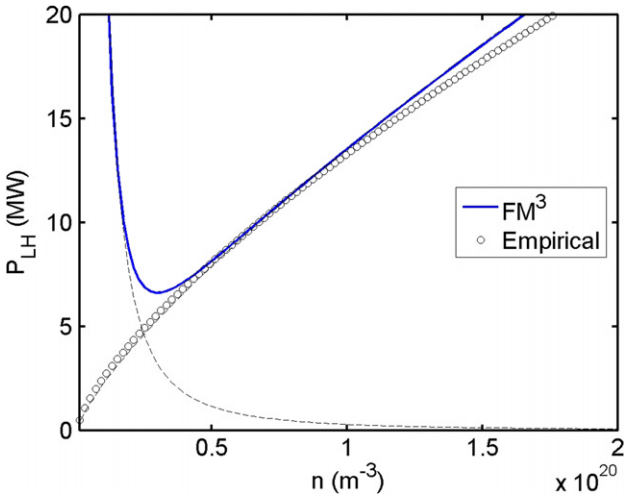

Figure 2. Predicted variation of $P_{\rm L–H}$ with plasma density for typical JET conditions. Also shown are the low and high density asymptotes, and the empirical prediction, (1).

To eliminate $T_{\rm e\star}$, we combined (17) and (19) to find an explicit expression for the SOL upstream temperature, and hence for $T_{\rm e\star} \approx T_{\rm e\odot} = T_{\rm eu}$,

$$T_{\rm e\star} \approx T_{\rm e\odot} \approx \left[\left(\frac{P_{\rm L–H}}{S_\parallel} \frac{1}{\gamma \zeta n_{\rm et}} \right)^{\frac{7}{3}} + \frac{7}{4} \frac{P_{\rm L–H} L_\parallel^\odot}{\kappa_{0\rm e} S_\parallel} \right]^{\frac{2}{7}}. \tag{24}$$

The two terms appearing in (24) correspond to two distinct regimes of SOL transport: the left term dominates in the sheath limited (or low recycling) regime in which $1 < T_{\rm eu}/T_{\rm et} < 2$, and the right in the conduction limited (or high recycling) regime, $T_{\rm eu}/T_{\rm et} > 2$. The transition between these two regimes, defined as the point at which $T_{\rm eu}/T_{\rm et} \approx 2$, occurs at some critical value of the SOL collisionality, typically at $\nu_\odot \approx 15$ (note that $10 < \nu_\odot < 80$ are typically found on tokamaks) [26]. The resulting variation in predicted $P_{\rm L–H}$ is shown in figure 2 for typical JET conditions ($R = 3\,$m, $a = 1\,$m, $\kappa = 1.7$, $B = 3\,$T, $I_{\rm p} = 3\,$MA, $q_{\rm cyl} \approx 2.8$, $q_{95} \approx 3.6$, $A = 2$, $Z = 1$, $L_{\rm p} \approx 2.8\,$cm, $\lambda_q \approx 1.8\,$cm) and free parameters chosen as $\alpha_\star \approx 24$, $\alpha_\odot \approx 2.6$.

In the *conduction limited* regime, i.e. for $\nu_\odot \gg 15$, when $T_{\rm eu}^{7/2} \gg T_{\rm et}^{7/2}$, (24) becomes

$$T_{\rm e\star}^{\rm cd} \approx T_{\rm e\odot}^{\rm cd} = T_{\rm eu}^{\rm cd} \approx \left[\frac{7}{4} \frac{P_{\rm L–H} L_\parallel^\odot}{\kappa_{0\rm e} S_\parallel} \right]^{\frac{2}{7}}. \tag{25}$$

Combining (25), (16) and (20), and simplifying yields,

$$P_{\rm L–H}^{\rm cd} \propto (n_{\rm e\star} B / \sqrt{A} q_\star)^{\frac{7}{9}} (R\epsilon)^{\frac{16}{9}} \kappa^{\frac{1}{2}} q_\odot^{\frac{5}{9}} (Z/A)^{\frac{1}{9}} Z^{\frac{5}{9}} \nu_\odot^{-\frac{5}{9}}. \tag{26}$$

Since the $P_{\rm L–H}$ size scaling is generally reported in terms of $S_\perp$ rather than R, it is useful to express the minor radius, $R\epsilon = a$, in terms of the surface area, $S_\perp$, (13), which gives $a = R\epsilon \propto (S_\perp \epsilon)^{1/2} \kappa^{-1/4}$. Inserting this form into (26), introducing dependence of $q_\star$ (8) and $q_\odot$ (7) on the plasma current via $q_{\rm cyl}$, and noting that $\nu_\star / \nu_\odot \propto q_\star / q_\odot \propto q_{\rm cyl}^{-1/2}$, we find

$$P_{\rm L–H}^{\rm cd} \propto (n_{\rm e\star} B)^{\frac{7}{9}} (S_\perp \epsilon)^{\frac{8}{9}} \kappa^{\frac{1}{18}} g^{\rm cd}(A, Z) h^{\rm cd}(q_{\rm cyl}, \nu_\odot). \tag{27}$$

Table 1. Predicted scaling exponents at low, medium and high densities, and experimental ones at high density [3–5].

Quantity: $P_{LH} \propto$	Model ($\nu_\odot \ll 15$)	Model ($\nu_\odot \approx 15$)	Model ($\nu_\odot \gg 15$)	Experiment ($\nu_\odot > 15$)
B	3	1.4	0.78	0.82
n_e	−2	0	0.78	0.72
$S_\perp$	−0.5	0.5	0.89	0.94
ϵ	2	1.9	0.89	≈1
κ	0.055	0.055	0.055	≈0
δ	0	0	0	≈0
q_{cyl}	−0.75	−0.3	0.16	≈0
$q_\star$	−1.5	−1.4	−0.78	<0
$q_\odot$	0	0.4	0.55	>0
A	2	0.2	−0.5	≈ − 1
Z	−2.25	−0.15	0.66	0.7 (Z_{eff})

$$g^{cd}(A, Z) = (Z/A)^{\frac{1}{9}} A^{-\frac{7}{18}} Z^{\frac{5}{9}} = A^{-1/2} Z^{2/3}, \quad (28)$$

$$h^{cd}(q_{cyl}, \nu_\odot) = q_\star^{-\frac{7}{9}} q_\odot^{\frac{5}{9}} \nu_\odot^{-\frac{5}{9}} \propto q_{cyl}^{\frac{1}{6}} \nu_\odot^{-\frac{5}{9}}. \quad (29)$$

A similar calculation in the *sheath limited* regime, i.e. for $\nu_\odot \ll 15$, when $T_{e\star} \approx T_{eu}$, (24) reduces to T_{et} (19) yields

$$P_{L-H}^{sh} \propto n_{e\star}^{-2} B^3 S_\perp^{-\frac{1}{2}} \epsilon^{\frac{9}{2}} \kappa^{\frac{3}{4}} g^{sh}(A, Z) h^{sh}(q_{cyl}, \nu_\odot). \quad (30)$$

$$g^{sh}(A, Z) = (A/Z)[A/(Z+1)]^{\frac{5}{2}} A^{-\frac{3}{2}} \approx A^2 Z^{-9/4}, \quad (31)$$

$$h^{sh}(q_{cyl}, \nu_\odot) = q_\star^{-3/2} \nu_\odot^{-5}. \quad (32)$$

The low and high density asymptotic scalings are summarized in table 1. The latter are in good agreement with the observed P_{L-H} scaling exponents at high density (1) also shown in table 1. The model also reproduces the (generally observed) weak scaling of P_{L-H} with q_{cyl}, i.e. with I_p for fixed B_T, and predicts an inverse scaling with q_{cyl} at the lowest densities. The predicted scalings with $q_\star$ and $q_\odot$ are qualitatively consistent with the observed dependence of P_{L-H} on limiter versus divertor SOL, i.e. much higher in the former,

$$P_{L-H}^{lim} / P_{L-H}^{div} \approx (q_\star^{lim} / q_\star^{div})^{-7/9} \gg 1, \quad (33)$$

on single versus double null configurations, i.e. higher in the former [29, 32, 33]

$$P_{L-H}^{SND} / P_{L-H}^{DND} \approx (q_\star^{SND} / q_\star^{DND})^{-7/9} \sim (1/2)^{-7/9} \approx 1.7, \quad (34)$$

and on the divertor leg length, i.e. increasing with distance from X-point to target [34, 35],

$$P_{L-H} \propto L_\parallel^{5/9} \propto q_\odot^{5/9}, \quad (35)$$

Finally, the model predictions are also consistent with the observed hysteresis in access power, with $P_{H\to L} < P_{L\to H}$,

$$P_{H\to L} / P_{L\to H} \approx (L_p^{H\to L} / L_p^{L\to H})^{1/2} < 1, \quad (36)$$

with the caveat that the model may no longer be valid following the L–H transition and hence may not be applicable to study the H → L back transition!

A comparison of the model predictions with experimental measurements of P_{L-H} on several tokamaks, obtained from the ITPA L–H transition database, is shown in figure 3 (right frame); also shown is the comparison of the database with the best-fit power law scaling (1) (left frame), see [5]. Combined, the two figures indicate good agreement between the model, the empirical scaling and the multi-machine database. While not presented here, sensitivity analysis revealed this good agreement to be *highly insensitive* to the scaling exponents in (7) and (8), i.e. to the assumed square-root and linear dependences of $q_\star$ and $q_\odot$ on q_{cyl}, respectively. All the experimental results presented above, e.g. (1) and table 1, were obtained with a 'favourable' or 'forward' B_T direction, i.e. with $\boldsymbol{B} \times \nabla B$ pointing towards the X-point. A discussion of the effect of the toroidal field reversal on the L–H access power may be found in the appendix.

Since the scaling exponent of P_{L-H} with respect to density is negative at low density (sheath limited regime, $\nu_\odot \ll 15$), $P_{L-H} \propto n_{e\star}^{-2}$, and positive at high density (conduction limited regime, $\nu_\odot \gg 15$), $P_{L-H} \propto n_{e\star}^{0.78}$, this indicates that P_{L-H} has a minimum value at some intermediate density ($\nu_\odot \sim 15$) corresponding to the transition between these two regimes. This value, P_{L-H}^{min}, represents the minimum H-mode access power at any density (for specified values of all other parameters), and as such, is a very important quantity for any future tokamak reactor. The prediction of P_{L-H}^{min} and the corresponding density, $n_{e\star}^{min}$, is thus one of the key objectives of any mode of the L–H transition.

Inserting (24) into (16), differentiating with respect to density and simplifying, yields the scaling for the minimum H-mode access power,

$$P_{L-H}^{min} \propto B^{\frac{7}{5}} R \epsilon^{\frac{12}{5}} \kappa^{\frac{1}{2}} g_P(A, Z) h_P(q_{cyl}, \nu_\odot), \quad (37)$$

$$g_P(A, Z) = A^{\frac{1}{5}} Z^{\frac{1}{5}} (Z+1)^{-\frac{7}{10}}, \qquad h_P(q_{cyl}, \nu_\odot) = q_\star^{-\frac{7}{5}} q_\odot^{\frac{2}{5}} \nu_\odot^{-\frac{9}{5}} \propto q_{cyl}^{-\frac{3}{10}} \nu_\odot^{-\frac{9}{5}}. \quad (38)$$

The corresponding density is found to scale as

$$n_{L-H}^{min} \propto B^{\frac{4}{5}} R^{-1} \epsilon^{\frac{4}{5}} \kappa^0 g_n(A, Z) h_n(q_{cyl}, \nu_\odot), \quad (39)$$

where

$$g_n(A, Z) = A^{\frac{9}{10}} Z^{-\frac{3}{5}} (Z+1)^{-\frac{9}{10}}, \qquad h_n(q_{cyl}, \nu_\odot) = q_\star^{-\frac{4}{5}} q_\odot^{-\frac{1}{5}} \nu_\odot^{-\frac{8}{5}} \propto q_{cyl}^{-\frac{3}{5}} \nu_\odot^{-\frac{8}{5}}. \quad (40)$$

In view of the tokamak density limit, it is useful to normalize (39) by the Greenwald density, $n_{GW} \propto I_p/a^2$. Recalling (2), the resulting Greenwald fraction is found to scale

$$f_{GW,L-H}^{min} \propto B^{-\frac{1}{5}} R^0 \epsilon^{\frac{4}{5}} \kappa^{-1} g_f(A, Z) h_f(q_{cyl}, \nu_\odot), \quad (41)$$

where $g_f(A, Z) = g_n(A, Z)$ is the same as in (40) and

$$h_f(q_{cyl}, \nu_\odot) = h_n(q_{cyl}, \nu_\odot) q_{cyl} \propto q_{cyl}^{\frac{2}{5}} \nu_\odot^{-\frac{8}{5}}. \quad (42)$$

This prediction is in good agreement with the experimentally observed variation of $f_{GW,L-H}^{min}$, which is found to be roughly independent of R and to decrease weakly with B, see figure 4.

Finally, in order to test the assertion made earlier, that the transition between the sheath limited and conduction limited regimes (as represented by the two terms in (24)) occurs at a specified value of SOL collisionality, $\nu_\odot$, it is necessary to derive the scaling of $\nu_\odot$ at the minimum of P_{L-H}. This can be found by constructing $\nu_\odot$ from (39) and (24), with the following result:

$$\nu_{\odot,L-H}^{min} \propto B^0 R^0 \epsilon^0 \kappa^0 g_\nu(A, Z) h_\nu(q_{cyl}, \nu_\odot) \quad (43)$$

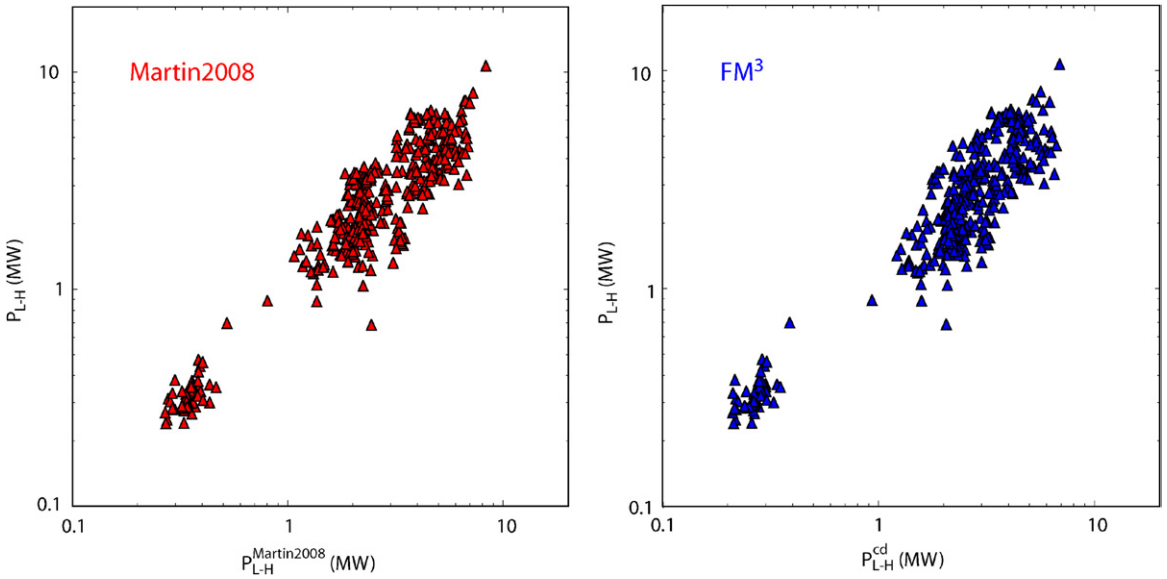

Figure 3. Comparison of experimental measurements of $P_{\mathrm{L-H}}$ on several tokamaks (ITPA data) with the best-fit scaling (left frame) (1) and the new model—labelled as FM^3 after the surnames of the authors—predictions (right frame).

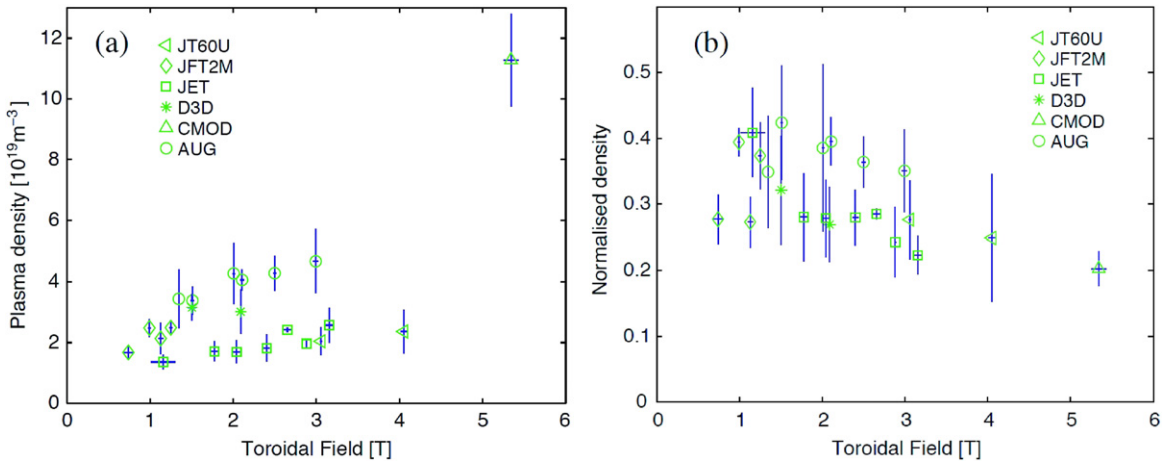

Figure 4. Variation of the measured minimum L–H access density (left frame) and the corresponding Greenwald fraction (right frame) with toroidal field. Reproduced with permission from [5]. © IOP Publishing.

and where

$$g_\nu(A,Z) = A^{\frac{1}{2}}(Z+1)^{-\frac{1}{2}}, \qquad h_\nu(q_{\mathrm{cyl}},\nu_\odot) = q_\star^0 q_\odot^0 \nu_\star^0 = 1. \tag{44}$$

Since most of the scaling exponents are zero, we may combine the above into a remarkable terse expression,

$$\nu^{\min}_{\odot,\mathrm{L-H}} \propto A^{\frac{1}{2}}(Z+1)^{-\frac{1}{2}} \tag{45}$$

which is a function of only A and Z. This result is entirely consistent with our expectations based on the two-point model, which predicts that the transition between sheath and conduction limited regimes occurs at constant collisionality for given A, Z [7, 26]. We note that for our reference set of parameters, $\nu^{\min}_{\odot,\mathrm{L-H}}$ is roughly 15, in broad agreement with the value suggested by the two-point model analysis [26]. In short, (45) suggests that the minimum H-mode access point indeed corresponds to the transition between the sheath and conduction limited regimes.

Acknowledgments

This work was funded by the RCUK Energy Programme under grant EP/I501045 and the European Communities under the contract of Association between EURATOM and CCFE. The views and opinions expressed herein do not necessarily reflect those of the European Commission.

Appendix

As a final remark, we consider the effect of the *relative* toroidal field direction on the L–H transition, which we have hitherto avoided in our discussion (all the experimental results presented above, e.g. (1) and table 1, were obtained with a 'favourable' or 'forward' B_{T} direction, i.e. with $\boldsymbol{B}\times\nabla B$ pointing towards the X-point). The relative B_{T} direction can be quantified by introducing the variable

$$\sigma_B = \mathrm{sign}\left[(\boldsymbol{B}\times\nabla B)\cdot(\boldsymbol{R}_X - \boldsymbol{R}_0)\right] \tag{46}$$

where $\boldsymbol{R}_X$ and $\boldsymbol{R}_0$ are position vectors of the X-point and plasma centre, respectively. Hence, σ_B measures the *direction* of $\boldsymbol{B} \times \nabla B$ vis-a-vis the position of the lower X-point (upper single-null results may be mapped to the lower single-null equivalent with a corresponding reversal of $\boldsymbol{B} \times \nabla B$, so that only lower single-null and double-null plasma need to be considered). Hence, $\sigma_B = 1$ for single null with forward B_T, -1 for single null with reverse B_T and 0 for symmetric double null (with either B_T direction). The effect of reversing the toroidal magnetic field, and hence flipping σ_B from 1 to -1, on the L–H transition is well documented: typically $P_{L–H}$ increases by a factor of 2–3 compared with the forward field case, e.g. see [29, 30, 32, 33]. This effect is absent from the model proposed above, which represents a balance of parallel and radial times, neither of which depends explicitly on σ_B. Nonetheless, it is likely that plasma quantities ($n_{e\star}$, $T_{e\star}$), their gradients (L_p, λ_q), the correlation length $L_\perp^{corr}$ and/or magnetic field quantities ($q_\star$, $q_\odot$) are in reality functions of σ_B, so that the predicted threshold power would change upon σ_B reversal. Indeed, the observed comparable increase of $P_{L–H}$ and $T_{e\star}$ [29, 30] when σ_B is flipped from 1 to -1 is consistent with (16).

The natural way to introduce the above dependence into the model is to make the free parameters $\alpha_\perp$, $\alpha_\star$ and $\alpha_\odot$ functions of σ_B[10]. The first of these represents the radial correlation length of the eddy, $L_\perp^{corr}$ in units of the meso-scale, $\sqrt{L_p \rho_S}$, see (9). Since the radial gradient (shear) in the $\boldsymbol{E} \times \boldsymbol{B}$ flow velocity tends to de-correlate (break-up) eddies and thereby reduce $L_\perp^{corr}$, we expect $\alpha_\perp$ to scale *inversely* with the magnitude of radial $\boldsymbol{E} \times \boldsymbol{B}$ shear, which is typically larger for $\sigma_B = 1$ than for $\sigma_B = -1$, e.g. see the measurements on Asdex Upgrade [32] (there are a number of possible reasons for this increase including asymmetries in the power flow and electron temperature in the SOL, see below). Noting that $P_{L–H} \propto L_\perp^{corr} \propto \alpha_\perp$, see (14), we would expect $P_{L–H}(\sigma_B = 1) < P_{L–H}(\sigma_B = -1)$ in agreement with the experiment.

The second parameter, $\alpha_\star$, represents the maximum safety factor in the edge region, $q_\star$, in units $\sqrt{q_{cyl}}$, see (7). Recalling the discussion of (7) and (8), we expect this quantity to be highly sensitive to the degree of magnetic stochasticity in the near-separatrix region (in contrast the third parameter, $\alpha_\odot$, which represents the maximum safety factor in the SOL region, $q_\odot$, in units q_{cyl}, see (8), is likely to be insensitive to σ_B). There are at least three separate effects by which the change in the σ_B would alter the degree of magnetic stochasticity and hence $\alpha_\star$:

- For $\sigma_B = 1$, the ratio of power deposited on the outer and inner targets is typically ≈ 3, and for $\sigma_B = -1$ it is close to unity. This translates into a strong outer : inner temperature asymmetry ($T_e^{out} \gg T_e^{in}$) and corresponding thermo-electric current between the two targets for $\sigma_B = 1$, and the near absence of such current for $\sigma_B = -1$; one would expect the change in this current to have a significant impact on the structure of the stochastic layer.
- For $\sigma_B = 1$ most of the SOL experiences a strong flow towards the inner target, with $M_\parallel \approx 0.3$ at the outer mid-plane and stagnation point at $\approx 45^\circ$ below the outer mid-plane, while for $\sigma_B = -1$ the flow is much more symmetric with $M_\parallel \approx -0.2$ at the outer mid plane and a stagnation point near the top of the vessel. Such flows can be expected to play a role in shielding the magnetic perturbations and changing the degree of stochasticity.
- Similarly, as already mentioned, $\boldsymbol{E} \times \boldsymbol{B}$ and diamagnetic drifts, whose sign is determined by that of σ_B, can directly impact on the eddy shearing rate, thus modifying the radial correlation length of the eddies, and potentially, the degree of stochasticity.

The combined effect of these three forces is beyond the scope of this work, and would require 3D resistive MHD simulations to quantify properly. Nonetheless, the model does allow us to make one concrete prediction in this regard, namely that $P_{L–H}$ is likely to be strongly affected by magnetic perturbations, which would modify $q_\star$ directly. This effect is easily testable and experiments are currently underway, e.g. on ASDEX Upgrade and MAST, to establish the influence of magnetic perturbations on the H-mode access power.

[10] Alternatively, one could adopt the approach used in fluid mechanics where the transition to turbulence is typically written as $Re > Re^*(Pr, Sc, shape, \ldots)$, i.e. with the critical Reynolds number being a weak function of the Prandtl, Schmidt, etc, numbers and the shape of the object considered. In our case, this would require that we modify (4) to read $Wa > Wa_{L–H}(\sigma_B)$. By choosing $Wa_{L–H}$ as a decreasing function of σ_B, the resulting $P_{L–H}$ could be reconciled with observations [29, 30].

References

[1] Wagner F. *et al* 1982 *Phys. Rev. Lett.* **49** 1408
[2] Burell K. *et al* 1992 *Plasma Phys. Control. Fusion* **39** 1859–69
[3] Doyle E. *et al* 2007 *Nucl. Fusion* **47** S18
[4] Connor J.W. and Wilson H. *et al* 1999 *Plasma Phys. Control. Fusion* **42** R1
[5] Martin Y. *et al* 2008 *J. Phys.: Conf. Ser.* **123** 012033
[6] Biskamp D. *et al* 2003 *Magnetohydrodynamics Turbulence* (Cambridge: Cambridge University Press)
[7] Fundamenski W. 2010 *Power Exhaust in Fusion Plasmas* (Cambridge: Cambridge University Press)
[8] Scott B.D. 2003 *Phys. Plasmas* **10** 963
[9] LaBombard B. *et al* 2008 *Phys. Plasmas* **15** 056106
[10] Kadomtsev B.B. 1965 *Plasma Turbulence* (New York: Academic)
[11] Scott B. 1997 *Plasma Phys. Control. Fusion* **39** 1635
[12] Rogers B.N. *et al* 1997 *Phys. Rev. Lett.* **79** 229
[13] Frisch U. 1995 *Turbulence* (Cambridge: Cambridge University Press)
[14] Davidson P.A. 2004 *Turbulence: An Introduction for Scientists and Engineers* (Oxford: Oxford University Press)
[15] Kerner W. *et al* 1998 *Contrib. Plasma Phys.* **38** 118
[16] Guzdar P.N. *et al* 2004 *Phys. Plasmas* **11** 1109
[17] Goldstein H. 1980 *Classical Mechanics* 2nd edn (New York: Addison–Welsey)
[18] Kolmogorov A.N. 1954 *Dokl. Akad. Nauk* SSR **98** 527
[19] Punjabi A., Verma A. and Boozer A. 1994 *J. Plasma Phys.* **52** 91
[20] Xu G.S. *et al* 2009 *Nucl. Fusion* **49** 092002
[21] Fundamenski W. 2008 *Fusion Sci. Technol.* **53** 1023
[22] Garcia O.E. *et al* 2007 *Plasma Phys. Control. Fusion* **49** 47
[23] Militello F. 2011 *Plasma Phys. Control. Fusion* **53** 095002
[24] Mossessian D.A. *et al* 2003 *Phys. Plasmas* **10** 689
[25] Asdex Team 1989 *Nucl. Fusion* **29** 1959

[26] Stangeby P.C. 2000 *The Plasma Boundary of Magnetic Fusion Devices* (Bristol: Institute of Physics Publishing)
[27] Spitzer L. and Härm R. 1953 *Phys. Rev.* **89** 977
[28] Braginskii S.I. 1965 *Rev. Plasma Phys.* **1** 205
[29] LaBombard B. *et al* 2004 *Nucl. Fusion* **44** 1047
[30] Hubbard A. *et al* 2007 *Phys. Plasmas* **14** 056109
[31] Asakura N. *et al* 2007 *J. Nucl. Mater* **363-365** 41–51
[32] Meyer H. *et al* 2005 *Plasma Phys. Control. Fusion* **47** 843
[33] Meyer H. *et al* 2006 *Nucl. Fusion* **46** 64
[34] Andrew Y. *et al* 2004 *Plasma Phys. Control. Fusion* **46** A87
[35] Gohil P. *et al* 2009 *Nucl. Fusion* **49** 115004
[36] Meyer H. *et al* 2008 *Plasma Phys. Control. Fusion* **50** 53